

# Surface plasmon resonances in the absorption spectra of nanocrystalline cupric oxide.

B.A. Gizhevskii<sup>a</sup> Yu.P. Sukhorukov<sup>a</sup> N.N. Loshkareva<sup>a</sup>  
A.S. Moskvina<sup>b</sup> E.V. Zenkov<sup>b</sup> E.A. Kozlov<sup>c</sup>

<sup>a</sup>*Institute of Metal Physics, Ural Division of Russian Academy of Sciences, 620219  
Ekaterinburg, Russia*

<sup>b</sup>*Ural State University, 620083 Ekaterinburg, Russia*

<sup>c</sup>*Russian Federal Nuclear Center - Institute of Technical Physics, 456770,  
Snezhinsk, Russia*

---

## Abstract

Optical absorption spectra of nanocrystalline cupric oxide CuO samples, obtained using the converging spherical shock wave procedure, reveal significant spectral weight red-shift as compared with spectra of single crystalline CuO samples. In addition, some of these samples manifest the remarkable temperature-dependent "peak-dip-hump" feature near 1.3-1.6 eV. The minimal model suggested to explain both effects implies the nanoceramic CuO to be a system of two species of identical metallic-like droplets with volume fractions  $p_1 \gg p_2$  and damping parameters  $\gamma_1 \gg \gamma_2$ , respectively, dispersed in an effective insulating matrix. In other words, both effects are assigned to the surface plasmon (Mie) resonances due to a small volume fraction of metallic-like nanoscale droplets with Drude optical response embedded in the bare insulating medium. Simple effective medium theory is shown to provide the reasonable description of the experimental spectra.

*Key words:* cuprates, nanoceramic, optical absorption, inhomogeneity, effective medium

---

## 1 Introduction

In the past decade a good deal of interest has renewed to the cupric oxide CuO, generally recognized as the prototype material of a broad family of strongly correlated (SC) oxides. It is now believed, that a considerable amount of data, obtained by means of different experimental techniques gives evidence of an intrinsic electron inhomogeneity of these materials. The stripe scenario gained the prime importance in the context, and the observation of stripes

in a representative set of HTSC's and non-superconducting oxides, including CuO (1) was reported.

The tendency toward the phase separation and insulator-to-metal transition upon the chemical substitution is observed in many cuprates. In optical experiments, different stages of this process manifest itself in a marked increase of the infrared (IR) absorption within the dielectric gap, and the subsequent formation of the low-energy tail due to the itinerant carriers. Such an evolution is clearly seen in doped HTSC's and manganites and a number of other SC oxides (2). In a series of papers (3) we proposed an unified concept of the inhomogeneity in doped SC oxides, treating it as a system of polar electron and/or hole centers, the preformed nanoscale hole-rich and hole-poor regions, where the breakdown of the uniform charge distribution and the stable disproportionation is favoured by the Jahn-Teller nature of Cu (Mn) ion. The quantitative description of optical absorption spectra of basic SC oxides such as  $\text{La}_{2-x}\text{Sr}_x\text{CuO}_4$  (4),  $\text{La}_{1-x}(\text{Ca},\text{Sr})_x\text{MnO}_3$  (5; 6) was made possible within the approach and the complex structure of IR spectra of these systems have been interpreted as the manifestation of geometric (surface plasmon) resonances. Moreover, it seems probable that SC oxides which ground state is a result of competition between two phases have to contain a certain volume fraction of the droplets of competing phase.

While the nature and the existence itself of this *intrinsic* inhomogeneity in SC oxides remains a hot debated issue, there are a number of experimental technique to induce the electronic inhomogeneity extrinsically. The comparison of the physical properties of SC oxides with a controllable *extrinsic* inhomogeneity and that of doped SC oxides is of especial interest, since it enables to draw the conclusions about the (presumably) intrinsic inhomogeneity in the latter and makes it possible to get insight into the underlying physics of the oxides and the insulator-to-metal transition. The similarity of the effects of intrinsic and extrinsic inhomogeneity, observed under different conditions, could support the existence of the competing phases, that always present in the SC oxides and evolving, when the doping and/or external influence suppress the stability of the parent ground state.

Below we address simple monoxide CuO which is believed to be a relevant model system for a wide series of SC cuprates. Earlier on we have performed a detailed study of optical absorption of nominally pure stoichiometric single crystalline CuO samples, as well the samples, exposed to the fluence of the neutrons, electrons, and  $\text{He}^+$ -particles (7; 8; 9). Here, as in the case of nonisovalent chemical substitution in other cuprates, the accumulation of the defects leads to the redshift of the fundamental band edge and the appearance of new absorption spectral features within the dielectric gap. Hereafter we present the results of the optical studies of a series of high density polydisperse CuO nanoceramics. This material belongs to the nanocrystal oxides, which are the

metastable highly imperfect systems with generally substantial stoichiometry violation, determined by the sample preparation procedure. They are likely to exhibit a strong spatial nonuniformity with a broad distribution of concentrations and the physical properties of the inhomogeneities, that makes it possible to speak about the extended phase separation. The optical data relevant to the systems under consideration remain scanty because of general difficulties of the investigations of strongly disordered materials, and on the other hand, due to the problems in the preparation of dense granular samples required for optical experiments. Thus, the optical studies of the nanocrystalline cupric oxide is of especial interest as a probe of the peculiarities of its energy spectrum and as a promising method of the detection of the phase inhomogeneity. The rest of the paper is organized as follow. In the next section the experimental details and obtained results are presented. The theoretical interpretation and conclusions are given in Secs. III. and IV.

## 2 Experiment

The nanoceramic CuO specimens have been obtained by the processing of a standard polycrystalline samples with the mean size of the grain varying from 5 to 20  $\mu\text{m}$  (10) using the converging spherical shock wave procedure (11). The noticeable strength and high density of the ceramics (that amounts to 99 % of that of the theoretical close-packed structure) makes it appropriate for the preparation of thin platelets of 40 - 70  $\mu\text{m}$  in thickness, suitable for the measurements of optical absorption. Three samples, henceforth denoted as No 1, 2 and 3, with the mean size of the grain equal to 20, 60 and 100 nm, respectively, have been investigated, the granularity being estimated using the scanning tunnel microscope and by the broadening of X-ray diffraction lines (XRD). The XRD data and the analysis of O  $K\alpha$  X-ray emission spectra (XES) attested all samples to be monophasic (12). The annihilation radiation angular correlations (ACAR) analysis gave evidence of a considerable concentration of the oxygen vacancies and their agglomerates at the boundaries of crystalline grains (13).

The measured absorption spectra  $K(\omega)$  are shown in Fig. 1, where the data are normalized to  $K(2.0\text{ eV})$ . It can be seen, that the spectra of nanogranular samples differ in many respects from those of CuO single crystals (8). The main peculiarity of the present spectra is a dramatic transfer of spectral weight from the fundamental band to lower energies. Similar effect has been previously observed also in the spectra of CuO after the electron and ion irradiation (7; 8; 9). More pronounced spectral redistribution in our case can be regarded as an evidence of a higher degree of the structure imperfection and inhomogeneity of the nanoceramics. While the fundamental band edge in pure CuO is known to be 1.45 eV for room temperature (14), the corresponding quantity for the

present inhomogeneous nanoceramics can hardly be ascertained.

The most striking peculiarity of the spectra (Fig. 1) is a fine oscillating structure, smooth or quite pronounced, that emerges near the fundamental band edge. This is most clearly observed in the spectrum of the sample 2, where a remarkable "peak-dip-hump" feature with three peaks resolved at 1.33, 1.55 and 1.82 eV. This feature manifests a puzzling temperature dependence, most distinctly observed in the spectrum of the sample 2 (panel B of Fig. 1): while clearly resolved at  $T = 295$  K, it completely disappears upon cooling to 80 K. It is worth noting that this behaviour is obviously incompatible with the excitonic picture.

While the shape of the spectral profile (Fig. 1) is ascertained with a high precision, the absolute value of the absorption can hardly be displayed as reliably. E.g., the intensity of the pronounced peak at 1.33 eV is of about  $2100 \text{ cm}^{-1}$ . Such a small absorption near the fundamental band edge is at variance to the values derived from the typical complex dielectric permittivity of insulating cuprates like CuO,  $\text{La}_2\text{CuO}_4$ , from where the values of  $K \sim 10^5 \text{ cm}^{-1}$  can be derived (15). However, the magnitude of the early reported absorption coefficient of the CuO polycrystals (16) is in a reasonable agreement with the present data. We believe, that such a discrepancy is primarily related to the differences of the techniques based on the transmittance and reflectance analysis. While inessential for an ideal uniform medium, it may become crucial and unavoidable for strongly disordered systems, where the surface and bulk properties of the sample can differ due to the variation of the concentration and the structure of the inhomogeneity. In fact, it is only possible to speak about the effective optical characteristics of inhomogeneous system, where the "physical" contribution, related to the energy band structure, can hardly be separated from the "geometrical" one, that reflects the subtleties of the the nanoscale structure of a particular sample. Thus, for example, it is difficult to derive the dielectric permittivity of strongly inhomogeneous film from the measurements of its optical density, because the effective optical path length can be strongly elongated due to multiple reflections accompanied by an intricate frequency dependence.

### 3 Discussion

Proceeding to the theoretic analysis of the findings of Sec. II, we firstly address the strong red-shift effect in the spectra of CuO nanoceramics, that could hardly be explained by simple manifestation of the lattice imperfection and points to a strong rearrangement of electronic structure. Taking into account the nanoscopic texture of the samples we can speculate that the anomalous spectral weight shift effect evidences the appearance of the highly polariz-

able, or metallic-like nanoscopic droplets with a pronounced low-energy optical response. The question of their microscopic nature is involved and is out of the scope of the present paper. Below we shall approximate their optical response by conventional Drude model with a rather wide distribution of effective plasma frequencies  $\omega_p$  and relaxation rates  $\gamma$ . Thus we assume the nanoceramic CuO samples to form a disordered insulating matrix with highly polarizable inclusions having a Drude-like optical response. We shall term them as metallic-like droplets, although, properly speaking, the character of their optical response near zero frequency and the dc conduction properties cannot be fixed proceeding from the available experimental data.

The optical properties of such a metal-insulator composite can be described in frames of the effective medium theory (17). The theory predicts the unconventional optical response of the insulating media with metallic inclusions due to the so-called surface plasmon (Mie, or geometric) resonances (17; 18), that have no counterpart in homogeneous systems. These arise as a result of resonant behaviour of local field in the granular composite system in presence of highly polarizable inclusions and are governed to a considerable extent by the shape of the grains. The frequency of geometric resonance is then easily obtained as the one at which the polarizability of small particle diverges. For the case of spherical metallic particles embedded in the insulating matrix with dielectric permittivity  $\varepsilon_d$  this leads to the equation:

$$\varepsilon(\omega)_{part.} + 2\varepsilon_d = 0, \quad (1)$$

whence the resonance frequency is

$$\omega_r = \frac{\omega_p}{\sqrt{1 + 2\varepsilon_d}}, \quad (2)$$

if the Drude's expression with the plasma frequency  $\omega_p$  is assumed for the embeddings and  $\varepsilon_d$  is constant.

Turning to the case of nanocrystalline CuO samples, an additional complication of the theoretical treatment imposed by the low symmetry of the monoclinic CuO unit cell is to be faced. However, in the present study we may benefit by the fine-grained structure of the samples, where all anisotropy is averaged out. Thus, in what follows, we shall deal with the scalar effective permittivity  $\varepsilon_{eff}(\omega)$ . To calculate this quantity in frames of effective medium theory, we made use of the familiar Maxwell-Garnett-type approximation, widely applied to the description of heterogeneous systems with the so called "cermet topology" (see, e.g. Ref. (19)), where the inclusions are completely surrounded by the host medium. It yields the following expression for  $\varepsilon_{eff}$ :

$$\varepsilon_{eff} = \frac{(1-p)\varepsilon_d + \sum_i \Delta_i \varepsilon_i}{(1-p) + \sum_i \Delta_i}, \quad (3)$$

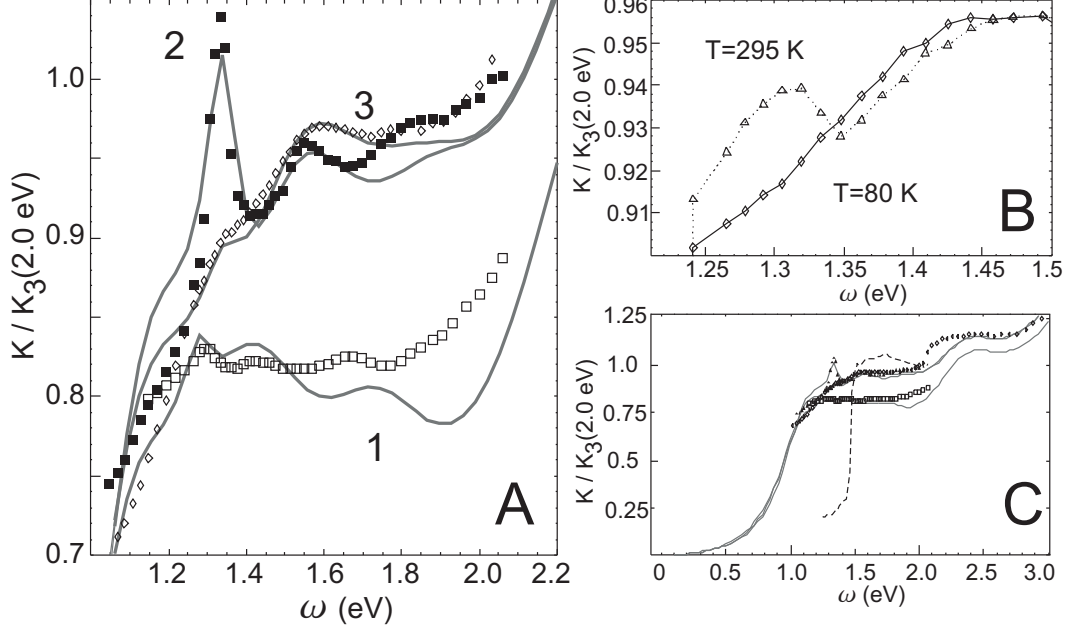


Fig. 1. A. Normalized room temperature absorption spectra of three CuO samples. Solid lines are the effective medium theory fits (details are given in the text). B. A fragment of the spectra of the sample 2, measured at two temperatures. C. The overall evolution of the spectra in the whole range considered. Dashed line marks the fundamental absorption band edge in pure CuO single crystal (8).

where

$$\Delta_i = \left\langle \frac{\varepsilon_i}{\varepsilon_d + L^{(i)}(\varepsilon_i - \varepsilon_d)} \right\rangle. \quad (4)$$

Here  $\varepsilon_d$  denotes the dielectric permittivity of the bare dielectric CuO medium,  $\langle \dots \rangle$  stands for the averaging over the inhomogeneity, including the distribution of the volume fractions  $p_i$ , orientations and other parameters, pertaining to different species of embeddings with dielectric permittivities  $\varepsilon_i$  and the principal values of the depolarization tensors denoted by  $L$ 's, overall concentration of inclusions being  $p$ . Thus, for a discrete set of species of randomly oriented embeddings,

$$\Delta_i = \frac{p_i}{3} \sum_{j=1}^3 \frac{\varepsilon_i}{\varepsilon_d + L_j^{(i)}(\varepsilon_i - \varepsilon_d)}, \quad \sum_i p_i = p, \quad (5)$$

where  $j$  runs over three depolarization factors of the grains of  $i$ -th species. Given the effective dielectric permittivity, the absorption coefficient is defined by the standard expression:

$$K(\omega) = 2 \frac{w}{c} \text{Im} \sqrt{\varepsilon_{eff}(\omega)}, \quad (6)$$

It is useful to observe, that the working form of the above expression, where  $K$  is measured in  $\text{cm}^{-1}$  and  $\omega$  in eV, is obtained by substitution  $2/c \rightarrow 101355$ .

The calculation of  $\varepsilon_{eff}$  with Eq.(3) requires the dielectric permittivities of the components to be specified. In practice, we are forced to make a number of strong simplifications and formulate a minimal model that yields the explanation of main experimental findings. A simple reasonable model implies the nanoceramic CuO to be a system of identical metallic droplets with volume fraction  $p$  dispersed in an effective insulating matrix. We simulated the dielectric CuO medium by the superposition of two Lorentz contributions:

$$\varepsilon_d = \varepsilon_\infty + \frac{1}{\pi} \sum_{k=1,2} \frac{I_k}{\omega_k^2 - \omega^2 - i\Gamma_k \omega}, \quad (7)$$

centered at  $\hbar\omega_1 = 2.35$  eV ( $\Gamma_1 = 0.9$  eV,  $I_1 = 14.256$ ) and  $\hbar\omega_2 = 4.5$  eV ( $\Gamma_2 = 0.9$  eV,  $I_2 = 469.8$ ), where  $I_k$  and  $\Gamma_k$  are the strength and the damping factor of  $k$ -th oscillator, respectively, and  $\varepsilon_\infty = 3.5$ . The permittivity of the metallic embeddings of  $i$ -th sort was described by a simple Drude formula,

$$\varepsilon_i = 1 - \frac{\Omega_{p,i}^2}{\omega(w + i\gamma_i)}. \quad (8)$$

This choice implies, that the characteristic transition energies of the novel metallic-like phase lie well below those of the insulating one. An important adjustable parameter, that can substantially affect the absorption spectrum, is the shape of inclusions, that enters the calculations through the depolarization factors (Eq. 5). Assuming the shapes to be ellipsoidal, we specified these with the ratios of two semi-axes to the third one, denoted by  $\alpha$  and  $\beta$ , respectively.

Although the data in Fig. 1 are presented in a dimensionless form, the model numerical calculations are possible given the absolute value of the absorption coefficient. However, as was pointed out in Sec. II, the artefact of the experimental procedure, based on the transmittance measurements near the fundamental band, results in a substantial underestimate of the magnitude of the absorption. In order to provide the description of the optical spectra of present cupric oxide nanoceramic, consistent with the experimental data available for other cuprates, such as  $\text{La}_2\text{CuO}_4$  (15), we multiplied the measured absorption coefficient by an arbitrarily chosen factor so as to set  $K \sim 10^5$   $\text{cm}^{-1}$  in the spectral range considered.

It is easy to see that choosing  $p \approx 20\%$ ,  $\omega_p \approx 4 \div 5$  eV,  $\gamma \approx 0.5$  eV,  $\alpha \approx 0.7$ ,  $\beta \approx 1.6$  we arrive at a reasonable description of the spectra of all the samples excluding the "peak-dip-hump" feature revealed in sample 2. At first sight, its natural explanation might be related to the exciton effects. However, this conventional approach encounters troubles, because no similar feature of comparable strength are observed in nominally pure CuO single crystals, and above all, because of its quite unusual temperature dependence, depicted in panel B of Fig. 1, where it is clearly seen, that peak near 1.3 eV, being very sharp at the room temperature (295 K), rapidly decays and finally disappears

Table 1

Fit parameters of the metallic-like droplets for the samples No. 1-3.

No	$p_1$	$\Omega_p^{(1)}$	$\gamma^{(1)}$	$\alpha_1$	$\beta_1$	$p_2$	$\Omega_p^{(2)}$	$\gamma^{(2)}$	$\alpha_2$	$\beta_2$
1	0.186	4.35	0.45	0.72	1.45	0.0265	4.25	0.02	1.6	1.6
2	0.201	4.75	0.5	0.73	1.6	0.0084	4.75	0.01	1.9	1.9
3	0.20	4.75	0.5	0.73	1.6	0.0042	4.75	0.07	1.9	1.9

upon cooling to 80 K that is incompatible with the excitonic picture.

At the same time, we believe, that the most plausible model of these phenomena should take into account the correlation of the observed spectral features and the effects of inhomogeneity in different microgranular samples. The close examination of the spectra and their comparison with the absorption spectrum of nominally pure cuprates make it possible to conclude, that the inclusions present in the samples are not monodisperse, but include several fractions with distinctly different properties which simplified averaging can provide only a "coarse-grained" description. In our approach, the existence of rather narrow spectral feature, strongly marked in the spectrum 2, points to a sizeable volume fraction of droplets with "good" metallic properties, or small magnitude of damping parameter  $\gamma$ . Among its most probable origins we consider e.g. the precipitation of Cu nanograins under the influence of an intense spherical shock waves, leading to the accumulation of numerous point and linear defects. Indeed, the macroscopic concentration of Cu has been previously found in cupric oxide after the fast particle irradiation (9) and plastic deformation (20). The measurements of the photoelectron Cu 2*p* spectra (XPS) also give evidence of a number of the copper ions Cu<sup>+</sup> with the reduced valency, that amounts to a few percents, although this is at variance to the XRD and XES data on the monophasic structure of the sample, reported above. Thus, to fit the fine resonant structure, clearly discernible in the spectra 1, 2, 3, we introduced the simplest possible spread of the inhomogeneity structure by considering two species of metallic-like droplets with volume fractions  $p_1 \gg p_2$  and damping parameters  $\gamma_1 \gg \gamma_2$ , or "bad" and "good" metal, respectively. The fitted parameters for all the samples are listed in Table I. Of course, the physical parameters of the particulate phases do not directly compare with their "bulk" counterparts, e.g. due to the quantum size effect, that becomes important for small particles in the size range below 100 nm (17).

The comparison of the theoretical curves with experiments shows, that the resonant structure of the absorption spectra, that evolve into the quite pronounced "peak-dip-hump" feature in the spectrum 2, can be naturally assigned to the Mie resonance.

We note the striking sensitivity of theoretical spectra to the variation of the parameters of the inhomogeneity, and especially to those of the phase with



small damping constant. The slightest changes in the relative volume fractions of two sorts of inclusions result in a dramatic effects in the absorption spectra. This can reasonably account for the difference in the spectra of the samples 2 and 3, because a subtle variation of the parameters from sample to sample is practically unavoidable. Such a variation of the internal texture of the inhomogeneity can be driven also with the temperature. It is clearly observed in the panel B of the Fig. 1, where a fragment of the absorption spectrum of the sample 2 is depicted for two temperatures. Some discrepancy of the present data with those of the main panel is due to the differences in the experimental techniques, employed in both cases. It can be clearly seen, that the pronounced peak at 1.34 eV in the room-temperature spectrum completely disappears under cooling. Interestingly, the spectra of the sample 2 measured at  $T=80$  K look quite similar to the room temperature spectra of the sample 2 and 3. The effective medium approach makes it possible to reproduce the essential features of experimental spectra slightly varying the model parameters. The effect of the temperature can be ascribed mainly to the changes in the relative volume of the second ("good") component. We have found, that the reduction of the relative volume of the highly polarizable phase with the lowering the temperature by less than 8 % is enough to simulate such a singular temperature behaviour. To get insight into the underlying mechanism of this volume fraction effect, we note the onset of 3D antiferromagnetic order in CuO, that takes place near  $T \sim 230$  K. In general, the onset of antiferromagnetism at low temperatures is expected to entail the suppression of the metallic-like phase. The way this occurs may be either the direct reduction of the volume fraction and/or the changes in the properties of the droplet. Moreover, the volume effect can be accompanied also by the deformation of conducting inclusions, that results in some shift and possible splitting of the geometric resonances, thus contributing to the broadening of the feature, observed in the 295 K spectrum. We regard its unusual temperature dependence as an important signature to its "geometric" nature.

Within the conventional effective medium approach, the inclusions are assumed to be much smaller, than the wavelength, and behave as the point electric dipoles. No other Mie resonances besides the first one (electric dipole) can be obtained within the model. To take into account the finite size of the inclusions, higher order terms of the Mie series are to be involved in the calculation of  $\varepsilon_{eff}$ . In a dilute limit, this step beyond the conventional effective medium scheme can be implemented using the expression:

$$\varepsilon_{eff} = \varepsilon_d \left( 1 - \frac{3ip}{(\omega/c)^3} S(0) \right), \quad S(0) = \frac{1}{2} \sum_n (a_n + b_n) \quad (9)$$

where  $S(0)$  is the forward scattering cross-section of spherical particle and the Mie's coefficients  $a_n, b_n$  are the functions of  $\varepsilon_d, \varepsilon_i$  and the particle diameter to the wavelength ratio,  $x$ . For  $x \gtrsim 1$ , the absorption spectra acquire a fine

ripple structure, related to the multipole excitations of the spherical particle. We made use of the Eq.(9) to check on, whether the three distinct observed feature of the absorption coefficient (Fig.1) could be related to the high-order Mie oscillations. It was found, that the observed features could in fact be explained not only as due to three different dipole resonances of an ellipsoidal particle, but as a result of the consecutive multipole resonances of a spherical particle. However, in order the latter conclusion to be true, the improbably large particles radii ( $\sim 1550$  nm) are required. A possible way to get round this difficulty is to suggest the aggregation of the nanoscale inclusions. Recent numerical extension of the Mie theory to the clusters of spherical inclusions (21) demonstrate the spectacular oscillations of the extinction coefficient of such aggregates.

#### 4 Conclusion

In conclusion, the optical absorption of nanocrystalline CuO samples have been studied in spectral range  $1 \div 3$  eV. We found the pronounced spectral weight red-shift as compared with the spectra of single crystalline CuO samples. In addition, the samples manifest the fine spectral structure, such as a remarkable temperature-dependent "peak-dip-hump" feature near  $1.3 \div 1.6$  eV. The minimal model suggested to explain both effects implies the nanoceramic CuO to be a system of two species of metallic-like droplets with volume fractions  $p_1 \gg p_2$  and damping parameters  $\gamma_1 \gg \gamma_2$ , respectively, dispersed in an effective insulating matrix. In other words, both effects are assigned to the surface plasmon (Mie) resonances due to a small volume fraction of metallic-like nanoscale droplets with Drude optical response embedded in the bare insulating medium. Theoretical analysis within the effective medium framework is shown to provide a good semi-quantitative agreement with experiment. We underline the striking sensitivity of the optical response to the variation of the metallic volume fraction and other effective medium parameters, especially to those of the "good" metal phase. The slightest unavoidable changes in the relative volume fractions of two sorts of inclusions from sample to sample and with the temperature result in dramatic effects in the absorption spectra. Finally, we would like to emphasize a clear similarity of the optical response produced by the extrinsic nanoscale inhomogeneity created in different way (the shock wave as in present study, the different irradiation) and intrinsic nanoscale inhomogeneity created by a chemical doping in parent insulating cuprates. This supports the idea of phase instability of these SC oxides with regard to the nucleation of metallic-like phase, or phase separation.

## Acknowledgements

The work was supported by INTAS 01-0654, CRDF No. REC-005, Federal Program (Contract No. 40.012.1.1. 1153-14/02), grants RFBR No. 01-02-96403, No. 02-02-96404, RFMC No. E00-3.4-280 and UR 01.01.042.

## References

- [1] X. G. Zheng, C. N. Xu, Y. Tomokiyo, E. Tanaka, H. Yamada, and Y. Soejima. *Phys. Rev. Lett.*, **85** (2000) 5170
- [2] S. Uchida, H. Eisaki and S. Tajima. *Physica C* **186-188** (1993) 975
- [3] A.S. Moskvin. *Physica B* **252** (1998) 186, and refs. therein.
- [4] A. S. Moskvin, E. V. Zenkov and Yu. D. Panov. *J. Luminescence* **94-95** (2001) 163
- [5] A. S. Moskvin, E. V. Zenkov, Yu. D. Panov, N. N. Loshkareva, Yu. P. Sukhorukov, and E. V. Mostovshchikova. *Phys. Sol. State* **44** (2002) 1519
- [6] Yu.P. Sukhorukov, N.N. Loshkareva, E.A. Gan'shina, E.V. Mostovshchikova, I.K. Rodin, A.R. Kaul, O.Yu. Gorbenko, A.A. Bosak, A.S. Moskvin, E.V. Zenkov. *JETP* **123** (2003) 293
- [7] N.N. Loshkareva, Yu.P. Sukhorukov, S.V. Naumov, B.A. Gizhevskii, T.A. Belykh, G.N. Tatarinova. *Phys. Sol. State* **41** (1999) 1433.
- [8] N.N. Loshkareva, Yu.P. Sukhorukov, B.A. Gizhevskii, S.V. Naumov, A.V. Kar'kin. *Zhurnal Tekhnicheskoy Fiziki* **69** (1999) 98.
- [9] Yu.P. Sukhorukov, N.N. Loshkareva, A.S. Moskvin, V.L. Arbuzov, S.V. Naumov. *Pis'ma v Zhurnal Tekhnicheskoy Fiziki* **24** (1998) 7.
- [10] B.A. Gizhevskii, E.A. Kozlov, A.E. Ermakov, N.V. Lukin, S.V. Naumov, A.A. Samokhvalov, V.L. Arbuzov, K.V. Shalnov, M.V. Degtyarev. *Phys. Met. Metallorg.* **92** (2001) 153.
- [11] E.A. Kozlov, E.V. Abakshin, V.I. Tarzhanov. Russian Federation Patent No 2124716 of December 24, 1997.
- [12] B.A. Gizhevskii, V.R. Galakhov, D.A. Zatsepin, L.V. Elokhina, T.A. Belykh, E.A. Kozlov, S.V. Naumov, V.L. Arbuzov, K.V. Shalnov, M. Neumann. *Phys. Sol. State* **44** (2002) 1380.
- [13] A.P. Druzhkov, B.A. Gizhevskii, V.L. Arbuzov, E.A. Kozlov, K.V. Shalnov, S.V. Naumov and D.A. Perminov. *J. Phys.: Condens. Matter* **14** (2002) 7981.
- [14] Yu.P. Sukhorukov, N.N. Loshkareva, A.A. Samokhvalov, A.S. Moskvin. *JETP* **108** (1995) 998.
- [15] S. Uchida, T. Ido, H. Takagi, T. Arima, Y. Tokura, S. Tajima. *Phys. Rev. B*, **43** (1991) 7942
- [16] F. Marabelli, G.B. Parravicini and F. Salghetti-Drioli. *Phys. Rev. B*, **52** (1995) 1433

- [17] David J. Bergman and David Stroud, in: H. Ehrenreich and D. Turnbull, Eds., *Solid State Physics* **46** (1992) 148.
- [18] H.C. van de Hulst, *Light Scattering by Small Particles* (Wiley, New York 1967).
- [19] W. Lamb, D.M. Wood, and N.W. Ashcroft. *Phys. Rev. B*, **21** (1980) 2248.
- [20] D.A. Zatsepin, V.R. Galakhov, B.A. Gizhevskii, E.Z. Kurmaev, V.V. Fedorenko, A.A. Samokhvalov, and S.V. Naumov. *Phys. Rev. B*, **51** (1999) 211.
- [21] F.J. García de Abajo, *Phys. Rev. B*, **60** (1999) 6086.